Dynamically slow processes in supercooled water confined between hydrophobic plates

2009 J. Phys.: Condens. Matter 21 504107

(http://iopscience.iop.org/0953-8984/21/50/504107)

IOP Publishing Journal of Physics: Condensed Matter

J. Phys.: Condens. Matter **21** (2009) 504107 (9pp) doi:10.1088/0953-8984/21/50/504107

Dynamically slow processes in supercooled water confined between hydrophobic plates

Giancarlo Franzese[1] **and Francisco de los Santos**[2]

[1] Departamento de Física Fundamental, Universidad de Barcelona, Diagonal 647, Barcelona 08028, Spain
[2] Departamento de Electromagnetismo y Física de la Materia, Universidad de Granada, Fuentenueva s/n, 18071 Granada, Spain

E-mail: gfranzese@ub.edu and fdlsant@ugr.es

Received 2 June 2009, in final form 16 July 2009
Published 23 November 2009
Online at stacks.iop.org/JPhysCM/21/504107

Abstract

We study the dynamics of water confined between hydrophobic flat surfaces at low temperature. At different pressures, we observe different behaviors that we understand in terms of the hydrogen bond dynamics. At high pressure, the formation of the open structure of the hydrogen bond network is inhibited and the surfaces can be rapidly dried (dewetted) by formation of a large cavity with decreasing temperature. At lower pressure we observe strong non-exponential behavior of the correlation function, but with no strong increase of the correlation time. This behavior can be associated, on the one hand, to the rapid ordering of the hydrogen bonds that generates heterogeneities and, on the other hand, to the lack of a single timescale as a consequence of the cooperativity in the vicinity of the liquid–liquid critical point that characterizes the phase diagram at low temperature of the water model considered here. At very low pressures, the gradual formation of the hydrogen bond network is responsible for the large increase of the correlation time and, eventually, the dynamical arrest of the system, with a strikingly different dewetting process, characterized by the formation of many small cavities.

(Some figures in this article are in colour only in the electronic version)

1. Introduction

1.1. Supercooled water and polyamorphism

Supercooled water is a metastable state of liquid water with respect to crystal ice and occurs when H_2O is cooled slowly below the freezing point. It can be easily prepared by cooling relatively pure commercial water and is commonly observed in nature, especially under confinement, as for example in plants where water is still liquid at $-47\,^{\circ}$C. It may crystallize into ice by catalysts, such as an ice crystal, or by a large exchange of mechanical energy, such as a strong vibration. However, without catalysts or external work, it is a useful example of a liquid whose dynamics slows down when the temperature decreases toward the homogeneous nucleation temperature T_H (with $T_H = -41\,^{\circ}$C at 1 atm and $T_H = -92\,^{\circ}$C at 2000 atm) [1]. The study of supercooled water is important in the long-lasting efforts to understand the physics of the hydrogen bonds, which characterize water and are the origin of its unique properties [2].

Below T_H water crystallizes, but a fast quench from ambient T to $T < T_X = -123\,^{\circ}$C (at 1 atm) freezes the liquid into a disordered (not crystalline) ice, leading to the formation of (amorphous) glassy water [3]. By increasing the pressure it has been observed that glassy water changes from low density amorphous (LDA) to high density amorphous (HDA) [4] and from HDA to very high density amorphous (VHDA) [5]. Therefore, water shows polyamorphism and this phenomenon has been related to the possible existence of more than one liquid phase of water [6]. Other thermodynamically consistent scenarios have been proposed, such as a first-order liquid–liquid phase transition with no critical point [7] or the absence of liquid–liquid phase transition itself [8], and their experimental implications are currently debated [9].

1.2. Confined water

Confinement is an effective way to suppress the crystal nucleation. Water molecules in plants, rocks, carbon nanotubes, living cells or on the surface of a protein, are confined to the nanometer scale. The effect of the confining surface on the properties of water is the object of intensive theoretical and numerical research (e.g. see [10–12]) and many recent experiments show a rich phenomenology which is the object of intense debate (e.g. see [7, 13–21]). The relation between the properties of confined and bulk supercooled water is not fully understood, therefore it is useful to elaborate handleable models that could help in developing a consistent theory.

1.3. Models for water

Since experiments in the supercooled region are difficult to perform, numerical simulations play an important role in the interpretation of the data. These simulations are based on models with different degrees of detailed description and complexity. Among the most commonly used, there are the ST2 [22] (two positive and two negative charges in a tetrahedral position plus a central Lennard-Jones, or LJ), the SPC and its modification SPC/E (three negative and one positive charges plus a central LJ) [23], the TIP3P, TIP4P, and TIP5P with three, four and five charges, respectively [24], the models with internal degrees of freedom [25], polarizability [26] and three-body interactions [27], and *ab initio* models for the evaluation of the significance of quantum effects [28, 29].

Models with increasing detail lead to improved accuracy in the simulations, but suffer from important technical limitations in the time and size of the computation. Due to their complexity, an analysis of how each of their internal parameters affects the properties of the model is in general very computationally expensive and a theoretical prediction of their behavior is unfeasible, limiting their capacity to offer an insight into unifying concepts in terms of universal principles, and hampering their ability to study thermodynamics properties.

On the other hand, simplified theoretical models, such as the Ising model, can be very drastic in their approximations, but are able to offer a general view on global, and possibly universal, issues such as thermodynamics and dynamics. They can be studied analytically or by simulations, providing theoretical predictions that can be tested by numerical computation. Therefore, they offer a complementary approach to the direct simulation of detailed models. Their characterization in terms of a few internal parameters make them more flexible and versatile, offering unifying views of different cases. Their study by theoretical methods, such as the mean field, leads to analytic functional relations for their properties, allowing one to predict their behavior over all the possible values of the external parameters. Their reduced computational cost permits direct testing of the theoretical forecasts in any condition. Furthermore, their study helps in defining improved detailed models for greater computational efficiency. Therefore, there is a strong need for simplified models of water that can keep the physical information and provide a more efficient simulation tool.

In the following we will describe a simple model for water in two dimensions (2D). The model can be easily extended to 3D, however here we consider only the 2D case. It can be thought of as a monolayer of water between two flat hydrophobic plates where the water–wall interaction is purely repulsive (steric hard-core exclusion). It has been shown that the properties of confined water are only weakly dependent on the details of the confining potential between the smooth walls and that the plate separation is the relevant parameter determining whether or not a crystal forms [30]. The case we consider here corresponds to the physical situation in which the distance between the plates inhibits the crystallization. We will analyze the dynamics of the system and the hydrophobic dewetting (or drying) process of the surface, consisting in the appearance of cavities, as recently observed in simulations for hydration water on protein surfaces [11] or nanopores [31].

2. Cooperative cell model confined between partially hydrated hydrophobic plates

2.1. General definition of the model

Cell models with variable volume are particularly suitable to describe fluids at constant pressure P, temperature T and number of molecules N, as in the majority of experiments with water. Here we consider a cell model based on the idea of including a three-body interaction, as well as an isotropic and a directional term for the hydrogen bonds [32, 33]. The three-body term takes into account the cooperative nature of the hydrogen bond. This model reproduces the experimental phase diagram of liquid water [34, 35] and, by varying its parameters, the different scenarios for the anomalies of water [36, 37].

We consider water confined between two hydrophobic plates within a volume V that accommodates N molecules. To minimize the boundary effects, we consider double periodic boundary conditions. We assume that the distance between the plates is such that water forms a monolayer, similar to the one observed in molecular dynamics simulations for TIP5P [38] and SPC/E [11] water, where each water molecule has at most four nearest neighbors. The system is divided into L^2 cells of equal volume $v = V/L^2$. Differently from previous works on this model [2, 9, 32–37, 39, 40], here we consider partially hydrated walls with a hydration level corresponding to a water concentration of 75% with respect to the available surface of one wall. This concentration is well above the site percolation threshold (59.3%) on a square lattice [41]. We assume that in each cell $i = 1, 2, \ldots, L^2$ there is at most one water molecule and we assign the variable $n_i = 1$ if the cell is occupied, and $n_i = 0$ otherwise.

The water–water interaction is described by three terms. One takes into account all the isotropic contributions (short-range repulsion of the electron clouds, weak attractive van der Waals or London dispersion interaction, and strong attractive isotropic component of the hydrogen bond interaction). This term is given by a hard-core repulsion at a distance $R_0 = v_0^{1/2}$

plus an LJ potential

$$U(r) = \begin{cases} \infty & \text{for } r \leqslant R_0 \\ \epsilon\left[\left(\dfrac{R_0}{r}\right)^{12} - \left(\dfrac{R_0}{r}\right)^{6}\right] & \text{for } r > R_0, \end{cases} \quad (1)$$

where r is the distance between two molecules.

The second term takes into account the directionality of the hydrogen bond interaction. Each molecule participates in at most four hydrogen bonds when each donor O–H forms an angle with the acceptor O that deviates from linear (180°) within 30° or 40° approximately. To incorporate this feature in the model, we assign for each water molecule i four indices $\sigma_{ij} \in [1, 2, \ldots, q]$, one for each possible hydrogen bond with the four nearest neighbors molecules j. The parameter q is chosen by selecting 30° as the maximum deviation from the linear bond, hence $q = 180/30 \equiv 6$. With this choice, every molecule has $q^4 = 6^4 \equiv 1296$ possible orientations. This directional interaction can be accounted for by the energy term

$$E_J = -J \sum_{\langle i,j \rangle} n_i n_j \delta_{\sigma_{ij},\sigma_{ji}} = -J N_{\mathrm{HB}}, \quad (2)$$

where the sum runs over all nearest-neighbor cells, $J > 0$ is the energy associated with the directional component of the hydrogen bond, and N_{HB} is the total number of hydrogen bonds in the system.

As a consequence of their directionality, the hydrogen bonds induce a rearrangement of the molecules in an open network (tetrahedral in 3D), in contrast with the more dense arrangement that can be observed at higher T or higher P [42]. This effect can be included in the model by associating a small volume contribution v_{HB}, due to the formation of each bond, to the total volume of the system

$$V = V_0 + N_{\mathrm{HB}} v_{\mathrm{HB}} \quad (3)$$

where $V_0 = N v_0$ is the volume of the liquid with no hydrogen bonds.

Finally, experiments show that the relative orientations of the hydrogen bonds of a water molecule are correlated [43]. As an effect of the cooperativity between the hydrogen bonds, the O–O–O angle distribution becomes sharper at lower T [15]. Therefore, the accessible q values are reduced. We include this effect in the model through the energy term

$$E_\sigma = -J_\sigma \sum_i n_i \sum_{(k,l)_i} \delta_{\sigma_{ik},\sigma_{il}}, \quad (4)$$

where J_σ is the energy gain due to the cooperative ordering of the hydrogen bonds, $(k, l)_i$ stands for the 6 different pairs of bond indices (arms) of a molecule i. At low T this term induces the reduction of accessible values of q (orientational ordering). In the limiting case, $J_\sigma = 0$, there is no correlation between bonds [8]. This case corresponds to considering as negligible the observed change in O–O–O angle distribution with T. The case $J_\sigma \gg 1$ corresponds to a drastic reduction of orientational states for the molecule from q^4 to q, with all the relative orientations between the hydrogen bonds kept fixed independently from T and P.

2.2. The parameters dependence of the phase diagram of the model

The complete enthalpy for the fluid reads

$$H = U(r) + E_J + E_\sigma + PV. \quad (5)$$

Each of the energy terms of (5) provides an energy scale, and depending on their relative importance different physical situations emerge. For instance, the choice $J < \epsilon$ guarantees that the hydrogen bonds are mainly formed in the liquid phase. As shown in [37], when $J_\sigma = 0$ the model gives rise to the scenario with no liquid–liquid coexistence [8]; at larger J_σ/J the model displays the scenario with a liquid–liquid critical point at positive pressure [6]; a further increase of J_σ/J brings it to a liquid–liquid critical point at negative pressure [44]; finally a further increase of J_σ/J brings it to the scenario where the liquid–liquid phase transition extends to the negative pressure of the limit of stability of the liquid phase [7].

The term

$$E_J + PV \equiv -(J - P v_{\mathrm{HB}}) N_{\mathrm{HB}} + P V_0 \quad (6)$$

is proportional to the number of hydrogen bonds N_{HB} and the associated gain in enthalpy decreases linearly with increasing pressure, being maximum at the lowest accessible P for the liquid, and being zero at $P = J/v_{\mathrm{HB}}$. For $P > J/v_{\mathrm{HB}}$ the formation of hydrogen bonds increases the total enthalpy.

In the following we choose $J/\epsilon = 0.5$, $J_\sigma/\epsilon = 0.05$, $v_{\mathrm{HB}}/v_0 = 0.5$ as in [34], for the sake of comparison. In the next sections we describe the simulation method adopted here and the results.

3. Kawasaki Monte Carlo method

Monte Carlo (MC) simulations are performed in the ensemble with constant N, P, T for $N = 1875$ water molecules distributed in a mesh of $L^2 = 2500$ cells, corresponding to 75% water concentration. We do not observe appreciable size effects at constant water concentration for ($N = 300$, $L^2 = 400$) and ($N = 1200$, $L^2 = 1600$). Preliminary results at 90% water concentration display no significant differences with the present case.

Since we are interested in studying the dynamic behavior of the system when diffusion is allowed, we adopt an MC method *a la* Kawasaki [45]. This method consists in exchanging the content of two stochastically selected nearest neighbor (n. n.) cells and accepting the exchange with probability

$$\begin{cases} \exp[-\Delta H/k_{\mathrm{B}}T] & \text{if } \Delta H > 0 \\ 1 & \text{if } \Delta H < 0 \end{cases} \quad (7)$$

where ΔH is the difference between the enthalpy (equation (5)) of the final state and the initial state.

The same probability is adopted for every attempt to change the state of any of the bond indices σ_{ij}. One MC step consists of $5N$ trials of exchanging n.n. cells i and j or changing the state of the bond indices σ_{ij} (every time

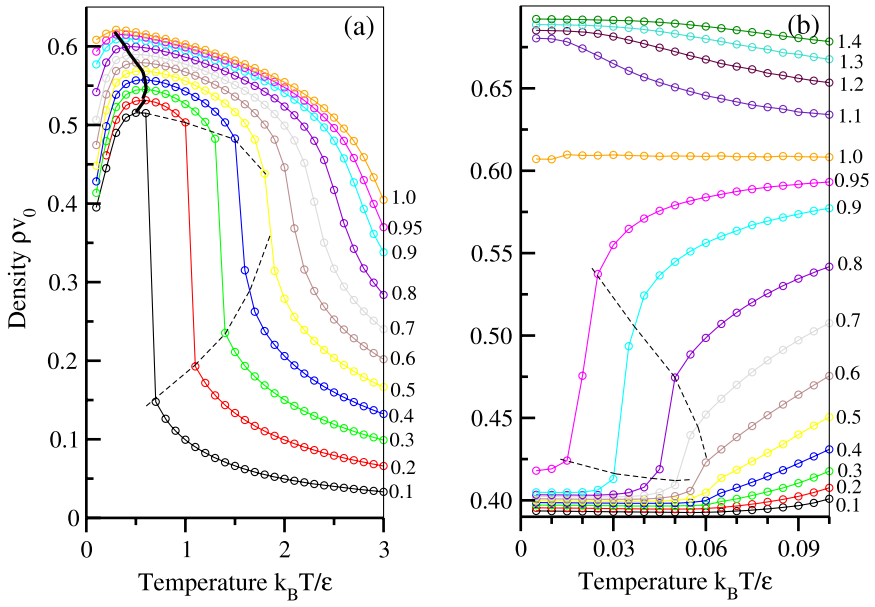

Figure 1. Density ρ of fluid water as function of temperature T at different values of pressure P, for $N = 1875$ water molecules distributed in $L^2 = 2500$ cells. The labels on the right of each panel are the values of Pv_0/ϵ of the nearest curve. (a) At high T a discontinuity in ρ appears below $Pv_0/\epsilon = 0.5$, marking the first-order phase transition between gas (at low ρ) and liquid (at high ρ), ending in a critical point at approximately $k_BT_C/\epsilon = 1.9 \pm 0.1$, $P_Cv_0/\epsilon = 0.50 \pm 0.05$. In the liquid phase, isobars show a temperature of maximum density (TMD line, marked by the thick black line) one of the characteristic features of water. (b) At low T the density rapidly decreases for $P < J/v_{HB} = 1\epsilon/v_0$. Finite size scaling analysis [34] shows that the decrease marks a first-order phase transition between high density liquid (at high ρ) and low density liquid (at low ρ), ending in the case considered here in a critical point at approximately $k_BT_{C'}/\epsilon = 0.06 \pm 0.01$, $P_{C'}v_0/\epsilon = 0.60 \pm 0.15$. In both panels, symbols are results of the MC calculation, lines are guides for the eyes, errors are comparable to the size of the symbols.

selecting at random which kind of move and which i and j are considered) followed by a volume change attempt. In the latter case, the new volume is selected at random in the interval $[V - \delta V, V + \delta V]$ with $\delta V = 0.5v_0$.

To avoid the interaction of a molecule with any other molecule, as it would be in the mean field, in the Lennard-Jones energy calculation we do not consider the volume changes due to the hydrogen bond formation. We allow the formation of hydrogen bonds independently from the size of the n. n. cells. We include a cut-off for the Lennard-Jones interaction at a distance equal to three times the size of a cell. Although with this choice the cut-off is density dependent, we tested that in this way we largely reduce the computational cost and that the results do not change in a significant way with respect to the case without the cut-off, due to the small variation of density in the liquid phase.

In the simulations we follow an annealing protocol, by preparing a random configuration and equilibrating it at high T and low P (gas phase). We equilibrate the system over 5×10^5 MC steps, and calculate the observable averaging over at least 2×10^6 MC steps. We use the final equilibrium configuration at a given temperature as the starting configuration for the next lower temperature.

4. Results and discussion

4.1. The phase diagram

Consistent with previous results based on finite size scaling analysis on the isothermal compressibility [34], from the discontinuity of the density at fixed P as function of T, we find a liquid–gas first-order phase transition ending in a critical point C at approximately $k_BT_C/\epsilon = 1.9 \pm 0.1$, $P_Cv_0/\epsilon = 0.50 \pm 0.05$ (figure 1(a)). In the liquid phase, we observe a temperature of maximum density (TMD) for any isobar with $Pv_0/\epsilon \leqslant 1$. This anomalous behavior in density is one of the characteristic features of water. Here we note that $Pv_0/\epsilon = 1$ corresponds to the limiting value $P = J/v_{HB}$ above which the formation of bonds increases the enthalpy in equation (6), consistent with the intuitive idea that the density maximum in water is a consequence of the open structure due to the hydrogen bond formation. For $P > J/v_{HB}$ the formation of hydrogen bonds is no longer convenient in terms of free energy and the system recovers the behavior of a normal liquid (with no open structures).

At lower T and for $P \leqslant J/v_{HB} = 1\epsilon/v_0$, the isobars display another rapid decrease between high density and low density (figure 1(b)), both at ρ higher than the gas density. As in the case with no diffusion [34], we associate this rapid decrease in ρ to a first-order phase transition between a high density liquid (HDL) and a low density liquid (LDL) ending in critical point C′ at $k_BT_{C'}/\epsilon = 0.06 \pm 0.01$ and $P_{C'}v_0/\epsilon = 0.60 \pm 0.15$. The values of the critical temperature for C′ is consistent, within the error bars, to that previously estimated [34, 33], while the value of $P_{C'}$ is somehow smaller, due to finite size effects that will be discussed in a future work. Here, instead, we focus on the analysis of the dynamics of the system at low T.

4.2. The dynamics at low temperature

To get an insight into the processes at low T associated with the hydrogen bond dynamics, we calculate the quantity $M_i \equiv \frac{1}{4}\sum_j \sigma_{ij}$, that gives the orientational order of the four bond indices of molecule i, and its correlation function

$$C_M(t) \equiv \frac{1}{N}\sum_i \frac{\langle M_i(t_0+t)M_i(t_0)\rangle - \langle M_i\rangle^2}{\langle M_i^2\rangle - \langle M_i\rangle^2} \qquad (8)$$

where the $\langle\cdot\rangle$ stands for the thermodynamic average [35, 36]. This correlator is the analogue of the self-dipole correlation function of water molecules, that has been shown [48] to be linearly related to the orientational autocorrelation function adopted to study the glassy behavior of the orientational degrees of freedom in supercooled water. It follows the standard definition of correlation functions for discrete (spin or orientational) variables (e.g. see [49] and references therein). To better see its physical meaning, we can consider its shifted value $M_i' \equiv M_i - (q-1)/2 \in [-(q-1)/2, (q-1)/2]$ and observe that at equilibrium $C_{M'}(t) \equiv C_M(t)$, with $\langle M_i'\rangle = 0$ when the molecule i has its bond indices in random states (as at high T), and $\langle M_i'\rangle = q^* - (q-1)/2 \neq 0$, when all its bond indices have the same integer value $q^* \in [1, q]$ (as at low T). The correlation function $C_M(t)$ is 1 at $t = 0$ and decays to 0 as soon as the variable M_i decorrelates from its value at t_0. Hence, $C_M(t) = 0$ for both randomized or fully ordered configurations, since in both cases $\langle M_i(t_0+t)M_i(t_0)\rangle = \langle M_i\rangle^2$, while it is $1 \geqslant C_M(t) > 0$ when the configurations at times t_0 and $t_0 + t$ are correlated. Its long-time limit gives the degree of arrest for the hydrogen bond dynamics as well as, for example, the density–density correlation function for the translational dynamics of supercooled liquids.

As we have discussed in the previous section, the effect of the hydrogen bond is evident only at pressure $P \leqslant J/v_{\mathrm{HB}}$ and below the TMD line. Therefore, we focus on state points at $P \leqslant 1\epsilon/v_0$ and $T \leqslant 0.4\epsilon/k_{\mathrm{B}}$.

- We first observe that for $P = 1\epsilon/v_0$ the correlation function is always exponential for all the temperatures with $0.005 \leqslant k_{\mathrm{B}}T/\epsilon \leqslant 0.4$ (△ in figure 2). From the exponential fits (dotted lines in figure 2) the characteristic decay time is $\tau \simeq 1.3$ MC steps (MCS) at $k_{\mathrm{B}}T/\epsilon = 0.4$, $\tau \simeq 2.2$ MCS at $k_{\mathrm{B}}T/\epsilon = 0.1$, and $\tau \simeq 10$ MCS at $k_{\mathrm{B}}T/\epsilon = 0.05$. Therefore, the correlation time increases by one order of magnitude for a decrease of T of one order of magnitude, but τ is always much shorter than the simulation time.
  This behavior is consistent with the observation of the typical configurations of hydrogen bonds at these P and T (upper row in figure 3). The water molecules condense on the hydrophobic surface, leaving a large dehydrated area (cavity), but the number of hydrogen bonds does not increase in an obvious way and no orientational order is observed even at the lowest T.
- Next, we decrease the pressure to $P = 0.7\epsilon/v_0$ (◇ in figure 2), close to the liquid–liquid critical pressure. At $k_{\mathrm{B}}T/\epsilon = 0.4$, the correlation function is exponential with $\tau \simeq 1$ MCS. At lower T the correlation function is no longer exponential. It can be well described with a stretched exponential function

$$C_M(t) = C_0 \exp\left[-(t/\tau)^\beta\right] \qquad (9)$$

where C_0, τ and $\beta \leqslant 1$ are fitting constant. For $\beta = 1$ the function is exponential, and the more stretched is the function, the smaller is the power $0 < \beta \leqslant 1$.
At $k_{\mathrm{B}}T/\epsilon = 0.1$, the stretched exponential (continuous line) has $\beta = 0.8$ and $\tau \simeq 3.1$ MCS, while at $k_{\mathrm{B}}T/\epsilon = 0.05$, the stretched exponential has $\beta = 0.4$ and $\tau \simeq 5$ MCS.
Hence, along isobars close to the liquid–liquid critical pressure, the dynamics of the liquid is not much slower than that at $Pv_0/\epsilon = 1$, but it becomes non-exponential below the TMD, a typical precursor phenomenon of glassy systems [46]. This phenomenology is usually associated with the presence of heterogeneity in the system. While in a homogeneous system the characteristic relaxation time is determined by some characteristic energy scale, in a heterogeneous system the presence of many characteristic energies induces the occurrence of many typical timescales, giving rise to a non-exponential behavior.
This is consistent with the increasing number of hydrogen bonds that can be observed at this pressure in the high density liquid phase (central panel on the second row in figure 3). The formation of many hydrogen bonds inhibits the free diffusion of the molecules, determining heterogeneities.
This effect is very obvious at the lower $k_{\mathrm{B}}T/\epsilon = 0.05$, where the non-exponential behavior of the correlation function is very strong ($\beta = 0.4$) and the hydrogen

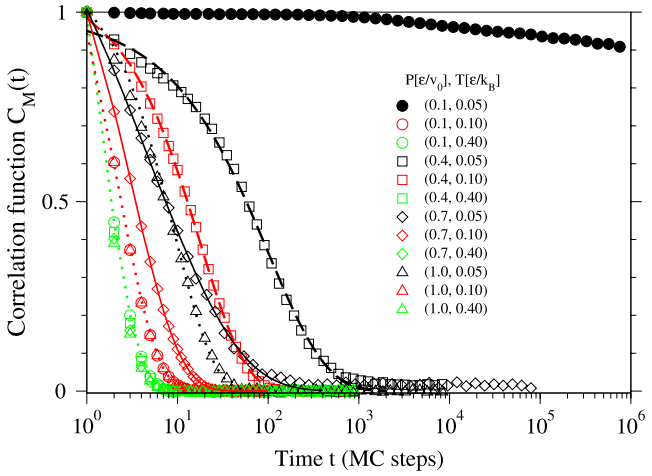

Figure 2. The correlation function $C_M(t)$ for different $P \leqslant 1.0\epsilon/v_0$ and $T \leqslant 0.4\epsilon/k_{\mathrm{B}}$ below the temperature of maximum density (TMD). The correlation decays as an exponential (dotted lines) at any $T \geqslant 0.4\epsilon/k_{\mathrm{B}}$ (not shown), just below the TMD, for any $P < 1.0\epsilon/v_0$ and for all T at $P = 1\epsilon/v_0$ (△). The correlation $C_M(t)$ is well described by a stretched exponential (equation (9)) for $P = 0.7\epsilon/v_0$ (◇, continuous line) and $P = 0.4\epsilon/v_0$ (□, dashed line) for $T \leqslant 0.1\epsilon/k_{\mathrm{B}}$ with a stretched exponent β that is larger at lower T. At low pressure $P = 0.1\epsilon/v_0$ (○), $C_M(t)$ is non-exponential only at very low $T = 0.05\epsilon/k_{\mathrm{B}}$ (●).

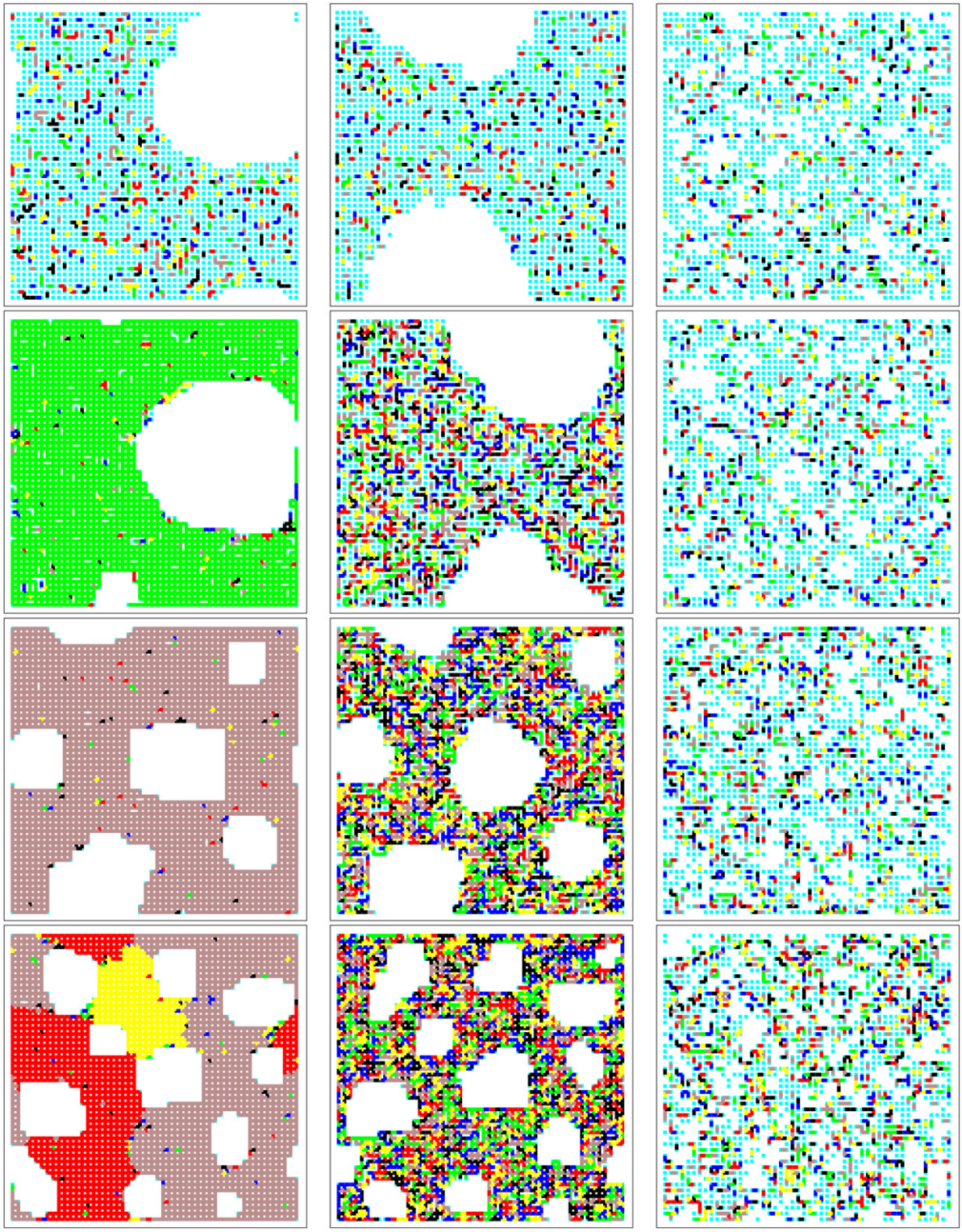

Figure 3. Hydrogen bond configurations showing the hydrogen bond ordering at low T and at $P < J/v_{\rm HB} = 1\epsilon/v_{\rm HB}$. Symbols: turquoise dots represent cells containing water molecules with at least one bond free; colored lines represent hydrogen bonds between molecules in n. n. cells, with six possible colors corresponding to the $q = 6$ possible values of the orientational state. Every row corresponds to a different P: from top to bottom, $P = 1\epsilon/v_0$, $P = 0.7\epsilon/v_0$, $P = 0.4\epsilon/v_0$, $P = 0.1\epsilon/v_0$. Every column corresponds to a different T: from right to left, $T = 0.4\epsilon/k_{\rm B}$, $0.1\epsilon/k_{\rm B}$, $0.05\epsilon/k_{\rm B}$. The size of the box is not in scale with the total volume of the system at the different values of P and T.

bond network is fully developed, but with many isolated locally disordered regions (left panel on the second row in figure 3). A typical configuration at low T at this P has the surface partially hydrated by low density liquid water (network of bonded molecules, marked in green in the panel). The network is almost complete, but many small

heterogeneities are present (marked with mismatching colors).

It is quite intriguing to observe that another mechanism that could be responsible (or co-responsible) for the stretching in the correlation function is the cooperative behavior of the system in the vicinity of the liquid–liquid critical point. If cooperative motions are necessary to rearrange the system and to allow the relaxation of the dynamics, a single timescale cannot be defined, resulting in a stretched decay of the correlation function. This is the usual reasoning in supercooled liquids, where it is possible to connect the cooperative motions (*cage effect*) with heterogeneities given by stringlike clusters of mobile particles, whose mean cluster size appears to diverge near the mode-coupling critical temperature [47]. In the present case the cooperativity is not on the translational degrees of freedom, but on the hydrogen bond dynamics. Considering that the hydrogen bond dynamics is experimentally accessible in confined systems at very low T, for example by dielectric relaxation spectroscopy [50], the analysis of its correlation time could represent the experimental probe for the liquid–liquid critical point that has been hankered for during the last two decades [6].

At this P the effect of the hydrogen bond network on dewetting starts to manifest itself. At low T, we observe the appearance of small cavities together with a main cavity. This indicates that the formation of the large hydrogen bond network inhibits the complete separation between the wet phase and the dewet (dry) phase.

- By further decreasing the pressure to $P = 0.4\epsilon/v_0$ (□ in figure 2), we observe an exponential decay of the correlation function at $k_BT/\epsilon = 0.4$ (dotted line) with $\tau \simeq 1.3$ MCS and a stretched exponential behavior (dashed line) when the liquid–liquid critical temperature is approached. Differently from the case at $P = 0.7\epsilon/v_0$, at $P = 0.4\epsilon/v_0$ the stretched exponent does not decrease in a strong way, but the relaxation time largely increases at lower T.

  In particular, at $k_BT/\epsilon = 0.1$, the stretched exponential has $\beta = 0.9$ and $\tau \simeq 18$ MCS, while at $k_BT/\epsilon = 0.05$, the stretched exponential has $\beta = 0.7$ and $\tau \simeq 100$ MCS. Therefore, the correlation time slows down by two order of magnitudes on decreasing T from $k_BT/\epsilon = 0.4$ to $k_BT/\epsilon = 0.05$.

  This different behavior with respect to the case at $P = 0.7\epsilon/v_0$ could be associated with the different evolution of the hydrogen bond network. Previous mean field [33] and MC results [2] have shown that the increase of the number of hydrogen bonds with decreasing T is much more gradual at low P than at high P. Therefore, at high P this process could generate quenched-in heterogeneities and strong non-exponentiality. At low P, instead, the gradual building up of the hydrogen bond network freezes the system, inducing a large slowing down. As a consequence, the system has large relaxation times, but the hydrogen bond network develops in a more ordered way (third row in figure 3).

Table 1. Correlation times τ (expressed in MC steps) and stretched exponents β, for different values of temperature T and pressure P. The exponent β is smaller for (T, P) closer to the liquid–liquid critical point C′ at $k_BT_{C'}/\epsilon = 0.06 \pm 0.01$ and $P_{C'}v_0/\epsilon = 0.60 \pm 0.15$, while the correlation time τ is larger at low P and T.

Fitting parameters (τ, β)			
	T (ϵ/k_B)		
P (ϵ/v_0)	0.05	0.10	0.40
1.0	(10, 1)	(2.2, 1)	(1.3, 1)
0.7	(5, 0.4)	(3.1, 0.8)	(1, 1)
0.4	(100, 0.7)	(18, 0.9)	(1.3, 1)
0.1	($>10^6$, $\leqslant 1$)	(2.2, 1)	(1.3, 1)

The gradual increase of the number of hydrogen bonds is also responsible for the slower dewetting of the hydrophobic surface. Many small cavities are annealed at a very slow rate by the progressive network formation, inducing a heterogeneous dewetting.

- We finally consider the lowest pressure $P = 0.1\epsilon/v_0$ (○ in figure 2). In this case, the correlation time is exponential (dotted line) for $k_BT/\epsilon = 0.4$ and $k_BT/\epsilon = 0.1$, with $\tau \simeq 1.3$ MCS and $\tau \simeq 2.2$ MCS, respectively.

  At these temperatures the system is homogeneous, with no order at $k_BT/\epsilon = 0.4$ (right panel on the bottom row in figure 3) and with small orientationally ordered regions at $k_BT/\epsilon = 0.1$ (central panel on the bottom row in figure 3). These regions are the effect of the slowly increasing number of hydrogen bonds N_{HB} and are possible only at low P, because only at low values of P is the enthalpy increase small, which is proportional to N_{HB} (equation (6)).

  As a consequence of the gradual increase of these locally ordered regions of bonded molecules, at lower T the system is trapped in metastable excited states where large regions of ordered bonded molecules, with different orientations, compete in their growth process (regions marked with different colors in the left panel on the bottom row in figure 3). This process resembles the arrested dynamics of other model systems for glassy dynamics [51]. It is characterized by a non-exponential correlation behavior, with characteristic times that are several order of magnitudes larger than those at slightly higher T. In our case the correlation time greatly exceeds the simulation time of 10^6 MCS (● in figure 2). The results on the correlation times τ and the stretched exponents β are summarized in table 1.

  As a consequence of the arrested dynamics, the dewetting process and the phase separation between the wet phase and the dewet phase are arrested. In these conditions, many small cavities are formed at intermediate T and frozen at the lowest T, with a relaxation time that is orders of magnitude longer than the simulation time.

5. Conclusions

We have studied the dynamics of the hydrogen bond network of a monolayer of water between hydrophobic plates at partial

hydration. We adopt a model for water with cooperative interactions [32, 40, 52]. The model can reproduce the different scenarios proposed for water [37]. We consider the parameters that give rise to a liquid–liquid phase transition ending in a critical point [34, 33]. It has been shown that in the supercooled regime, below the TMD line, the system has slow dynamics [2, 35, 36]. Here we adopt a diffusive MC dynamics to study the case at partial hydration.

Our results show a complex phenomenology. At high $P = 1\epsilon/v_0$ the effect of the hydrogen bond network is negligible due to the high increase of enthalpy for the hydrogen bond formation. This is reflected in the dynamics by a moderate increase of the correlation time, also at very low T. Therefore, the system reaches equilibrium easily. As a consequence, we typically observe the formation of a single large cavity responsible for the dewetting process.

At a pressure $P = 0.7\epsilon/v_0$, close to the liquid–liquid critical pressure, the rapid formation of the hydrogen bond network determines the presence of a large amount of heterogeneity in the system. As a consequence of this heterogeneity and of the cooperative behavior, characteristic of the dynamics in the vicinity of a critical point, the correlation function shows a strong non-exponential behavior at low T. Nevertheless, the correlation time does not increase in a large way, since the hydrogen bond network is fully developed only at very low T. Therefore, the dynamics relaxes within the simulation time and allows the formation of large cavities on the hydrophobic surface.

At lower $P = 0.4\epsilon/v_0$, the number of hydrogen bonds grows in a gradual and more homogeneous way when the temperature decreases. This process slows down the correlation decay by orders of magnitude. Nevertheless, the effect on the exponential character of the correlation function is small, because the system has only a small amount of heterogeneity and the cooperativity of the dynamics is small away from the liquid–liquid critical point. However, the effect on the process of surface dewetting is evident, with the formation of many small cavities.

This effect is extremely strong at very low $P = 0.1\epsilon/v_0$, where regions of ordered bonded molecules with different orientation grow in a competing fashion. This process give rise to an arrested dynamics, typical of many glassy systems, with a correlation time that increases by many orders of magnitude for a small decrease in temperature. The dewetting process in this case is almost completely frozen on the timescale of our simulations, with the formation of cavities with a broad distribution of sizes.

Acknowledgments

We thank our collaborators, P Kumar, M I Marqués, M Mazza, H E Stanley, K Stokely, and E G Strekalova, for discussions on different aspects of this topic. This work was partially supported by the Spanish Ministerio de Ciencia e Innovación Grant Nos. FIS2005-00791 and FIS2009-10210 (co-financed FEDER), Junta de Andalucía Contract No. FQM 357.

References

[1] Debenedetti P G and Stanley H E 2003 *Phys. Today* **56** 40–6
[2] Kumar P, Franzese G and Stanley H E 2008 *J. Phys.: Condens. Matter* **20** 244114
[3] Loerting T and Giovambattista N 2006 *J. Phys.: Condens. Matter* **18** R919–77
[4] Mishima O, Calvert L and Whalley E 1985 *Nature* **314** 76–8
[5] Loerting T, Salzmann C, Kohl I, Mayer E and Hallbrucker A 2001 *Phys. Chem. Chem. Phys.* **3** 5355–7
[6] Poole P, Sciortino F, Essmann U and Stanley H 1992 *Nature* **360** 324–8
[7] Angell C A 2008 *Science* **319** 582–7
[8] Sastry S, Debenedetti P G, Sciortino F and Stanley H E 1996 *Phys. Rev.* E **53** 6144–54
[9] Franzese G, Stokely K, Chu X Q, Kumar P, Mazza M G, Chen S H and Stanley H E 2008 *J. Phys.: Condens. Matter* **20** 494210
[10] Chandler D 2005 *Nature* **437** 640
[11] Giovambattista N, Lopez C F, Rossky P J and Debenedetti P G 2008 *Proc. Natl Acad. Sci. USA* **105** 2274–9
[12] Gallo P and Rovere M 2007 *Phys. Rev.* E **76** 061202
[13] Granick S and Bae S C 2008 *Science* **322** 1477
[14] Faraone A, Liu K H, Mou C Y, Zhang Y and Chen S H 2009 *J. Chem. Phys.* **130** 134512
[15] Ricci M A, Bruni F and Giuliani A 2009 *Faraday Discuss.* **141** 347–58
[16] Soper A K 2008 *Mol. Phys.* **106** 2053–76
[17] Bellissent-Funel M C 2008 *J. Phys.: Condens. Matter* **20** 244120
[18] Vogel M 2008 *Phys. Rev. Lett.* **101** 181801
[19] Pawlus S, Khodadadi S and Sokolov A P 2008 *Phys. Rev. Lett.* **100** 108103
[20] Mallamace F, Branca C, Broccio M, Corsaro C, Mou C Y and Chen S H 2007 *Proc. Natl Acad. Sci.* **104** 18387–91
[21] Chen S H, Liu L, Fratini E, Baglioni P, Faraone A and Mamontov E 2006 *Proc. Natl Acad. Sci. USA* **103** 9012–6
[22] Stillinger F and Rahman A 1974 *J. Chem. Phys.* **60** 1545
[23] Berendsen H, Grigera J and Straatsma T 1987 *J. Phys. Chem.* **91** 6269–71
[24] Jorgensen W, Chandrasekhar J, Madura J, Impey R and Klein M 1983 *J. Chem. Phys.* **79** 926–35
[25] Ferguson D 1995 *J. Comput. Chem.* **16** 501
[26] Jedlovszky P and Vallauri R 2005 *J. Chem. Phys.* **122** 81101
[27] Sprik M and Klein M 1988 *J. Chem. Phys.* **89** 7556
[28] Sprik M, Huttel J and Parrinello M 1996 *J. Chem. Phys.* **105** 1142
[29] Fernández-Serra M V and Artacho E 2008 *Phys. Rev. Lett.* **96** 016404
[30] Kumar P, Starr F W, Buldyrev S V and Stanley H E 2007 *Phys. Rev.* E **75** 011202
[31] Russo J, Melchionna S, De Luca F and Casieri C 2007 *Phys. Rev.* B **76** 195403
[32] Franzese G and Stanley H E 2002 *J. Phys.: Condens. Matter* **14** 2201–9
[33] Franzese G and Stanley H E 2007 *J. Phys.: Condens. Matter* **19** 205126
[34] Franzese G, Marqués M I and Stanley H E 2003 *Phys. Rev.* E **67** 011103
[35] Kumar P, Franzese G and Stanley H E 2008 *Phys. Rev. Lett.* **100** 105701
[36] Mazza M G, Stokely K, Strekalova E G, Stanley H E and Franzese G 2009 *Comput. Phys. Commun.* **180** 497–502
[37] Stokely K, Mazza M G, Stanley H E and Franzese G 2008 Effect of hydrogen bond cooperativity on the behavior of water, arXiv:0805.3468 [cond-mat]
[38] Kumar P, Buldyrev S V, Starr F W, Giovambattista N and Stanley H E 2005 *Phys. Rev.* E **72** 051503
[39] Franzese G, Yamada M and Stanley H E 2000 *3rd Tohwa University Int. Conf. on Statistical Physics*; *AIP Conf. Proc.* **519** 508–13

[40] Franzese G and Stanley H E 2002 *Physica* A **314** 508–13
[41] Chang K C and Odagaki T 1984 *J. Stat. Phys.* **35** 507–16
[42] Botti A, Bruni F, Ricci M A, Pietropaolo A, Senesi R and Andreani C 2007 *J. Mol. Liq.* **136** 236–40
[43] Kern C and Karplus M 1972 *Water: A Comprehensive Treatise* vol 1 (New York: Plenum) pp 21–91
[44] Tanaka H 1996 *Nature* **380** 328
[45] Kawasaki K 1972 *Phase Transitions and Critical Phenomena* vol 4 (London: Academic)
[46] Franzese G and Coniglio A 1999 *Phys. Rev.* E **59** 6409–12
[47] Donati C, Glotzer S C, Poole P H, Kob W and Plimpton S J 1999 *Phys. Rev.* E **60** 3107
[48] Kumar P, Franzese G, Buldyrev S V and Stanley H E 2010 *Phys. Rev.* E **73** 041505
[49] Franzese G 2000 *Phys. Rev.* E **61** 6383
[50] Mazza M G, Stokely K, Pagnotta S E, Bruni F, Stanley H E and Franzese G 2009 Two dynamic crossovers in protein hydration water and theirthermodynamic interpretation, arXiv:0907.1810 [cond-mat]
[51] Dawson K 2002 *Curr. Opin. Colloidal Interface Sci.* **7** 218–27
[52] de los Santos F and Franzese G 2009 *Modeling and Simulation of New Materials: Proc. Modeling and Simulation of New Materials: Tenth Granada Lectures*; *AIP Conf. Proc.* **1091** 185–97